Mechanical Systems and Signal Processing 159 (2021) 107800

Contents lists available at ScienceDirect

Mechanical Systems and Signal Processing

journal homepage: www.elsevier.com/locate/ymssp

Complete statistical approach to modelling variable pedestrian forces induced on rigid surfaces

M. García-Diéguez [a,*], V. Racic [b], J.L. Zapico-Valle [a]

[a] Department of Construction and Manufacturing Engineering, University of Oviedo, Campus de Gijón 7.1.21, 33203 Gijón, Spain
[b] Department of Civil and Environmental Engineering, Politecnico di Milano, Piazza Leonardo da Vinci 32, 20129 Milan, Italy

ARTICLE INFO

Article history:
Received 30 December 2019
Received in revised form 5 December 2020
Accepted 24 February 2021

Communicated by Dionisio Bernal

Keywords:
Footbridges
Floors walking
Gait variability
Vibration serviceability
Spatiotemporal parameters
Dynamic load factors

ABSTRACT

This study presents a stochastic model of near-periodic walking force signals featuring variable walking speed on the step-by-step basis as the key input modelling parameter. This is a notable departure from traditional deterministic and periodic Fourier series models where the key modelling parameter is the average pacing rate in a walking trial. Walking speed instead of pacing rate is a more natural choice since human nervous system adopts speed of successive steps to the surrounding environment, including vibrations of the supporting structure. Starting from the previously developed models of variable walking speed and spatiotemporal parameters in a walking trial, this study derived a complementary model of variable dynamic loading factors (DLFs) corresponding to the first five dominant harmonics and subharmonics of the walking force. Both the mean and coefficient of variation of DLFs are described as the products of two factors. The first represents the deterministic dependence on the step speed and is modelled as a second-order polynomial. The second factor reproduces the random inter-pedestrian variability of the DLFs which is defined by a Beta distribution. Extensive vibration simulations of virtual footbridges due to measured and simulated walking forces showed a reliable performance of the model. Moreover, the results provided a strong evidence that the step-by-step variability of gait in a single-pedestrian walking trial yields up to 22% relative error in the simulated vibration response.

1. Introduction

Vibration serviceability assessment governs design of contemporary pedestrian structures, such as footbridges and floors. Yet there is a total lack of quality models of pedestrian-induced loading that can be used to reliably predict vibrations at the design stage. The fact is reflected in dozens of vibration serviceability failures of newly built structures reported all around the world in the last two decades [1,2].

The leading guidelines for design of pedestrian structures portray individual pedestrian loading as deterministic and periodic time histories, thus described via Fourier series [2]. The relevant modelling parameters are pacing rate f_s and amplitudes of the first few dominant Fourier harmonics (typically up to four) that are functions of f_s. After scaling by the corresponding body weight, the Fourier amplitudes are commonly known as "dynamic loading factors" (DLFs). The corresponding phases are very little studied and usually neglected. DLF values adopted in the key design guidelines were derived from Kerr's exper-

* Corresponding author.
E-mail address: garciadmarta@uniovi.es (M. García-Diéguez).

https://doi.org/10.1016/j.ymssp.2021.107800
0888-3270/

iments featuring single footfalls recorded by a force plate mounted on a rigid laboratory floor [3]. More recent studies aimed to record continuously measured forces due to many successive steps. They measured the forces: (1) directly using instrumented treadmills [4–6], instrumented walkways [7] and foot-pressure insoles [8], and (2) indirectly using motion tracking technology, such as motion tracking markers [9,10], inertial sensors [11,12] and video cameras [13]. The continuously measured forces revealed the presence of subharmonics centred in-between the main harmonics. These are due to inborn asymmetry of gait, i.e. differences between the right and the left footfalls [14]. Although DLFs of subharmonics have smaller amplitudes than DLFs of the neighbouring harmonics, their energy is still high enough to create vibration serviceability issues [7]. This means that a reliable model of walking forces should not neglect them, as it is currently the case. The relevant guidelines favour walking frequency (also called pacing/footfall rate/frequency) rather than walking speed as the key force modelling parameter because the most severe load case scenario of pedestrian structures is a force harmonic matching a natural frequency of the structure yielding the resonance. While this sounds reasonable for a light pedestrian traffic, speed of walking rather than pacing rate is imposed to individuals in dense pedestrian crowds and is restrained by the crowd flow.

Human gait is characterised by great inter- and intra-pedestrian variability [2]. The former refers to differences between different individuals (usually called "test subjects" in experiments), while the latter means that a single person cannot make two identical successive footfalls, or it would be only by chance. Therefore, a stochastic rather than the deterministic modelling approach is more suitable to describe walking forces. However, stochastic models are still very rare and limited [5,15–17]. Even in deterministic characterisations inter-pedestrian variability is often recognised [18,19]. Intra-pedestrian variability is usually neglected as its influence on vibration response is traditionally labelled insignificant. However, more recent research showed that variability of pacing rate has a profound impact on the accuracy of predicted vibration levels [11,12,20,21]. Although models that include variability of pacing rate do exist [5,6], they commonly assume constant speed of walking. Extensive research in neurology and biomechanics of human gait proved that this is not how people actually walk [22]. Human nervous system controls speed rather than pacing rate during walking. People speed-up and slow-down while walking and interacting with their surrounding. Also, variations in other spatiotemporal gait parameters (including pacing rate) are adapted to the speed in such a manner to minimise the energy expenditure of walking [14].

In the previous studies, the authors derived statistical models of intra- and inter-pedestrian variability of walking speed for unrestricted walking [23] and other spatiotemporal parameters such as step length and step interval [24], both as functions of walking speed. Necessary details of these past studies needed in the present research are presented in Section 2. The aim of the present study is to provide a statistical model of variable DLFs as a function of walking speed, so it can be used in conjunction with these previously developed models to provide a comprehensive and reliable model of individual pedestrian loading.

The present study addresses DLFs of the first five dominant harmonics and subharmonics, thus covers the frequency range approximately between 0 and 12 Hz for the highest pacing rate 2.5 Hz [2]. It is assumed that the energy of the higher harmonics is not strong enough to induce significant resonant vibrations of footbridges and low-frequency floors [18,25]. Also, the study focusses on vibration response dominated by only one force harmonic or subharmonic. Under this condition, the relative phase of the (sub) harmonics has a negligible effect on the response. Hence, the phases are set to zero for all (sub) harmonics in each footfall.

The study is limited to walking on relatively rigid surfaces, i.e. when the vibration levels of the supporting structure are still not perceptible enough to change the usual gait pattern of healthy individuals. Variability of the gait parameters due to interaction with the neighbouring pedestrians [12,17] is out of the scope of this study. Interaction between the structure and a pedestrian is perceived only through the contact forces between the feet and the walking surface, generally known as ground reaction forces or GRFs [2]. Moreover, it is assumed that presence of a human body on the structure does not alter the dynamic properties of an empty structure. Hence, a phenomenon of human-structure dynamic interaction [26,27] is neglected in the present study. These limitations of the present research are due to the lack of adequate experimental data that would enable studying the selected gait parameters under the above mentioned circumstances. However, this research provides a universal analytical framework that can be used to study the modelling parameters based on any kind of the relevant gait data recorded for healthy individuals under various walking conditions, i.e. with or without perceptible structural motion or interaction with the surrounding people and environment.

2. Past models of key spatiotemporal gait parameters

The current study builds on the previously derived models of variable walking speed, step length, footfall interval and walking frequency [21,23,24]. These are all revised briefly in this section to enable a reader to follow developments presented in the rest of the paper. More detailed descriptions of the models and an instrumented treadmill designed and used to collect continuously measured vertical walking GRF signals, as well as experiments with a motion tracking system designed to study overground gait parameters can be found elsewhere [22,24]. Based on the force records from fifty test subjects (25 males and 25 females), 300 tests and more than 30 km of treadmill walking, the so established database of the vertical GRF measurements was also used in the present study (Section 3) to derive a model of variable DLFs needed to provide a comprehensive model of variable walking GRFs verified in Section 4.

2.1. Walking speed

Based on in situ measurements carried out at different geographical locations (Table 1), the average self-selected walking speed v among a population of healthy adults was found to fit well the Gaussian distribution. While this model accounts reliably for inter-pedestrian variability of the speed, it neglects intra-pedestrian variations for successive footfalls.

For unrestricted continuous healthy walking, speed v_i in each step i ($i = 1, 2, \ldots, N$) can be broken down into two components $v_i = \overline{v} + \tilde{v}_i$. Here, $\overline{v}$ is a constant (average) speed sampled from a Gaussian distribution of a kind given in Table 1 and $\tilde{v}_i$ is a random deviation described by the autoregressive model $\tilde{v}_i = c_1 \tilde{v}_{i-1} + c_2 \tilde{v}_{i-2} + w_i$. The autoregressive parameters c_1 and c_2 are independent of the average speed $\overline{v}$ and can be statistically described by a binormal distribution with the following mean μ and covariances Σ matrices:

$$\mu = \begin{bmatrix} 1.45 \\ -0.55 \end{bmatrix}, \quad \Sigma = \begin{bmatrix} 0.0210 & -0.0180 \\ -0.0180 & 0.0180 \end{bmatrix}. \tag{1}$$

The disturbances w_i are modelled as Gaussian white noise $w_i \sim \mathrm{N}(0, \sigma_w)$. The standard deviation σ_w is independent from $\overline{v}$ and can be sampled from the Beta distribution $B(17, 2103)$. In summary, the following steps determine a procedure to generate a sequence of speeds v_i in a single overground walking trial:

1. Define input data: mean, μ_v, and standard deviation, σ_v, of the average walking speed, $\overline{v}$, and the total number of steps, N, in the trial.
2. Sample a random value of the average speed, $\overline{v}$, from the distribution $N(\mu_v, \sigma_v)$.
3. Generate c_1 and c_2 by sampling from the binormal distribution defined in Eq. (1).
4. Check the stability of the autoregressive model. If $-1 > c_2 > 1$ or $c_1 + c_2 > 1$ or $c_2 - c_1 > 1$ go to Step 3; otherwise continue to Step 5.
5. Obtain the standard deviation of the disturbances, σ_w, by sampling from $B(17, 2103)$.
6. Obtain the disturbances, w_i, by sampling from the distribution $N(0, \sigma_w)$.
7. Calculate the step speed deviations by $\tilde{v}_i = c_1 \tilde{v}_{i-1} + c_2 \tilde{v}_{i-2} + w_i$, where $\tilde{v}_{-1} = \tilde{v}_{-2} = 0$.
8. Generate the step speed sequence adding the average speed to the previous deviations, $v_i = \overline{v} + \tilde{v}_i$.

2.2. Step length

Step length is correlated with walking speed via the empirical power law [24]:

$$\ell_s = c_3 v^{c_4}. \tag{2}$$

Here, c_3 and c_4 are parameters whose inter-pedestrian variability is described by a binormal distribution:

$$\mu = \begin{bmatrix} 0.586 \\ 0.463 \end{bmatrix}, \quad \Sigma = \begin{bmatrix} 0.0022 & -0.0015 \\ -0.0015 & 0.0062 \end{bmatrix}. \tag{3}$$

2.3. Footfall interval and frequency

2.3.1. Relationship with walking speed

Footfall (i.e. step) interval T and footfall (i.e. walking) frequency $f_s = 1/T$ are correlated with walking speed v via the well known relationship $v = \ell_s f_s = \frac{\ell_s}{T}$ [2]. Substituting it into the power law (2) yields the formulations $T = c_3 v^{c_4 - 1}$ and $f_s = \frac{1}{c_3} v^{1 - c_4}$.

Based on the statistical models of $\overline{v}, c_3$ and c_4 from the previous sections and extensive numerical simulations, it was demonstrated in [21] that the inter-pedestrian variability of the average footfall frequency is represented best by a log-normal distribution.

Table 1
Summary of inter-pedestrian variability of walking speeds after different authors.

Study	μ_v [m/s]	σ_v [m/s]	Country	No. Samples
Zivanovic [28]	1.39	0.20	Montenegro	2019
Pachi and Ji [29]	1.23–1.43	0.09–0.14	UK	800
Kasperski and Sahnaci [7]	1.38–1.51	–	Germany	6000
Chandra and Bharti [30]	0.97–1.36	0.19–0.22	India	1523
García and Zapico [24]	1.41	0.14	Spain	50

2.3.2. Inter and intra-pedestrian variability

Footfall intervals T_i of successive steps $i = 1, \ldots, N$ in a walking trial comprise an adaptive component $\overline{T}_i$ and a deviation $\widetilde{T}_i$, i.e. $T_i = \overline{T}_i + \widetilde{T}_i$. The adaptive component is correlated to the speed of walking made in each step v_i as $\overline{T}_i = c_3 v_i^{c_4 - 1}$. The deviation can be broken down into a deterministic part $\widetilde{T}_i^a$ due to inherent asymmetry of human gait and a random part $\widetilde{T}_i^r$, i.e. $\widetilde{T}_i = \widetilde{T}_i^a + \widetilde{T}_i^r$. The deterministic part is formulated as follows: $\widetilde{T}_i^a = c_{5i}(-1)^i$, where c_{5i} stands for the asymmetry of each step and is expressed as a function of the adaptive component of that step $c_{5i} = \frac{\overline{T}_i c_{n5}}{2}$. Parameter c_{n5} is the normalized asymmetry parameter and is constant in a trial. The inter-pedestrian variability of this parameter follows a Beta distribution $c_{n5} \sim B(2.67, 149.10)$. The random part is described by a second-order autoregressive model $\widetilde{T}_i^r = c_{6i}\widetilde{T}_{i-1} + c_{7i}\widetilde{T}_{i-2} + z_i$, where c_{6i} and c_{7i} are autoregressive parameters and z_i is a random disturbance. Each autoregressive parameter consists of a deterministic part described by a second-order polynomial and a random part: $c_{6i} = 0.0469\, v_i^2 - 0.0291\, v_i - 0.3448 + c_{n6}; c_{7i} = -0.0370\, v_i^2 - 0.0122\, v_i - 0.1545 + c_{n7}$. Random parts, c_{n6} and c_{n7}, are independent from the walking speed and follow symmetric Beta distributions: $c_{n6} \sim B(6.60, 6.60); c_{n7} \sim B(9.42, 9.42)$. The random disturbance of $\widetilde{T}_i^r$ is modelled as a Gaussian white noise $z_i \sim \mathrm{N}(0, \sigma_{z_i})$. The standard deviation $\sigma_{z_i} = c_8 (v_i^2 - 3.30\, v_i + 3.00)$ is a second-order polynomial, where c_8 is a random coefficient that follows Beta distribution $c_8 \sim B(14.15, 561.19)$.

2.3.3. Synthetic footfall intervals

For a given sequence of speeds, v_i, generated following the instructions given in Section 2.1, the corresponding sequence of footfall intervals, T_i, can be generated as:

1. Sample c_3 and c_4 from the binormal distribution defined by Eq. (3).
2. Compute the adaptive component, for each footfall, $\overline{T}_i = c_3 v_i^{c_4 - 1}$.
3. Sample normalised asymmetry parameter c_{n5} from the distribution B(2.67, 149.10).
4. Calculate the asymmetry parameter $c_{5i} = \frac{\overline{T}_i c_{n5}}{2}$.
5. Sample parameters c_{n6} and c_{n7} from distributions B(6.60, 6.60) and B(9.42, 9.42), respectively.
6. Compute the autoregressive parameters through equations $c_{6i} = 0.0469\, v_i^2 - 0.0291\, v_i - 0.3448 + c_{n6}$ and $c_{7i} = -0.0370\, v_i^2 - 0.0122\, v_i - 0.1545 + c_{n7}$.
7. Check stability of the autoregressive parameters: if $max(c_{7i}) > 1$ or $-1 > min(c_{7i})$ or $max(c_{6i}) + max(c_{7i}) > 1$ or $max(c_{7i} - c_{6i}) > 1$ go to Step 6; otherwise continue to Step 8.
8. Sample a random value of parameter c_8 from the distribution B(14.15, 561.19).
9. Compute the standard deviation of disturbances, $\sigma_{z_i} = c_8 (v_i^2 - 3.30\, v_i + 3.00)$.
10. Obtain the disturbance z_i by sampling from $N(0, \sigma_{z_i})$.
11. Calculate deviation of footfalls intervals, $\widetilde{T}_i = c_{5i}(-1)^i + c_{6i}\widetilde{T}_{i-1} + c_{7i}\widetilde{T}_{i-2} + z_i$ $(i = 1, 2, \ldots, N)$, where $\widetilde{T}_{-1} = \widetilde{T}_{-2} = 0$.
12. Generate the sequence of footfall intervals, $T_i = \overline{T}_i + \widetilde{T}_i$.

2.3.4. Position on structure

The pedestrian position x_i during step i $(i = 1, \ldots, N)$ along a walking path is commonly seen as the point of application of the footfall force. It can be described by the following equation:

$$x_i(t) = x_{i-1} + v_i t, \tag{4}$$

where x_{i-1} represents the position at the end of the step $i - 1$, $t = [0, T_i]$ and $x_0 = 0$. Generally speaking, x_i and v_i are vectors. As this study is limited to walking on flat horizontal surfaces, there are only two relevant vector components, both in the plane of a floor or a footbridge deck. However, in case of straight walking paths (which is usually the case in simulations), x_i is reduced only to one component, i.e. along the path.

Previous comparative studies between treadmill and overground walking [31–35] showed no statistically significant difference between the average values of the gait parameters in the two walking conditions. However, the intra-pedestrian variability of these parameters in the overground walking was found to be one order of magnitude higher than that of the treadmill walking [23]. It was also found that the relationship between the spatiotemporal parameters obtained in the treadmill walking can be extrapolated to the case of variable footfall speed measured overground. Therefore, it is reasonable to assume that a relationship between DLF amplitudes and walking speed derived from treadmill data can also be extrapolated to the case of overground speed. The next section starts from this premise.

3. Modelling variable DLFs

Each signal from the database of walking GRFs was normalised to body weight and cut into segments corresponding to both step and stride intervals. The segmentation was done in the same manner as in case of the analysis pertinent to the

force parameters described in Section 2, so the past and the current data analysis are compatible. Each segment corresponding to a step interval was run through the fast Fourier transform (FFT) algorithm to extract the amplitudes (i.e. DLFs) of the first five dominant Fourier harmonics. Moreover, the FFT is applied to the stride segments to get DLFs of the first five subharmonics. In the following sections, DLFs will be labelled $DLF_i^{(j)}$. The subscript indicates the step number in a sequence of N steps, i.e. $i = 1, \ldots, N$. The superscript $j = 1, \ldots, 5$ stands for the order of harmonics while $j = 0.5, \ldots, 4.5$ stands for the order of subharmonics.

The next two sections focus on deriving a "treadmill model" of a $DLF_i^{(j)}$ sequence. At this stage, the variability of walking speed on the step-by-step basis can be neglected. This means that in a walking trial the speed is assumed constant for all successive footfalls and is equal to the given constant speed of rotation of the treadmill belt [23]. The average value and variation of the DLFs in a trial are also considered constants, hence the fluctuation of the DLF values in a trial can be modelled as a stationary process. This "treadmill model" will be extended in Section 3.3 to "overground model", where both the average value and variation of the DLFs are functions of the variable speed for successive footfalls.

3.1. Preliminary data analysis

An example of a $DLF_i^{(j)}$ sequence across successive steps is illustrated in Fig. 1 for the second Fourier harmonic ($j = 2$). Based on a visual inspection, all other harmonics and subharmonics across all walking trials in the database show a similar random character.

$DLF_i^{(j)}$ can be broken down into two components: an average value $\overline{DLF}^{(j)}$ and random variations $\widetilde{DLF}_i^{(j)}$, i.e.

$$DLF_i^{(j)} = \overline{DLF}^{(j)} + \widetilde{DLF}_i^{(j)}. \tag{5}$$

$\overline{DLF}^{(j)}$ are not correlated with pedestrian body weight, which is in line with the findings reported elsewhere [5]. Also, variations $\widetilde{DLF}_i^{(j)}$ are not correlated either with variations of other (sub) harmonics and the corresponding variations of the footfall intervals $\widetilde{T}_i$. This means that $DLF_i^{(j)}$ can be studied independently from footfall intervals and other harmonics.

Fig. 2 shows the lack of interconnection between successive $\widetilde{DLF}_i^{(j)}$ values, which means that the current value of $\widetilde{DLF}_i^{(j)}$ in step i is independent from the values made in a few previous steps. Therefore, the variations can be considered a random process. The coefficient of variation is an easy way to quantify it:

$$CoV^{(j)} = \frac{S_{DLF}^{(j)}}{\overline{DLF}^{(j)}}, \tag{6}$$

where $S_{DLF}^{(j)}$ is a standard deviation of $DLF_i^{(j)}$.

$DLF_i^{(j)}$ values are in the range [0–1] and they fit well a Beta distribution $B(a, b)$ as shown in Fig. 3. Parameters a and b of the Beta distribution can be obtained from its mean μ and variance σ^2 [36] as:

$$a = \frac{\mu^2(1-\mu)}{\sigma^2} - \mu, \quad b = a\frac{1-\mu}{\mu}. \tag{7}$$

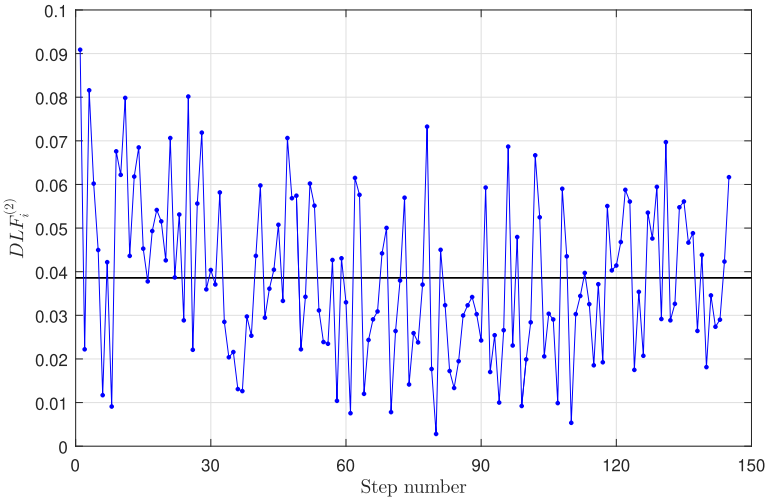

Fig. 1. $DLF_i^{(2)}$ values for successive steps. The horizontal line is the average value $\overline{DLF}^{(2)}$.

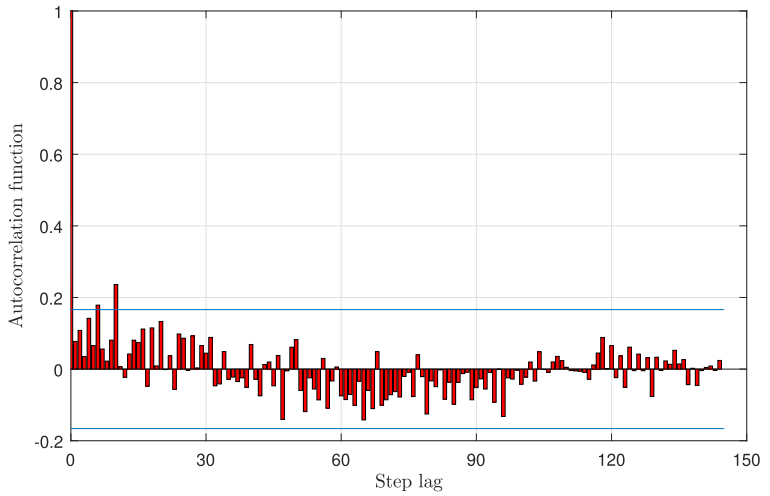

Fig. 2. Autocorrelation function of $\widetilde{DLF}_i^{(2)}$, corresponding to the data presented in Fig. 1. The horizontal lines are a 95% confidence interval.

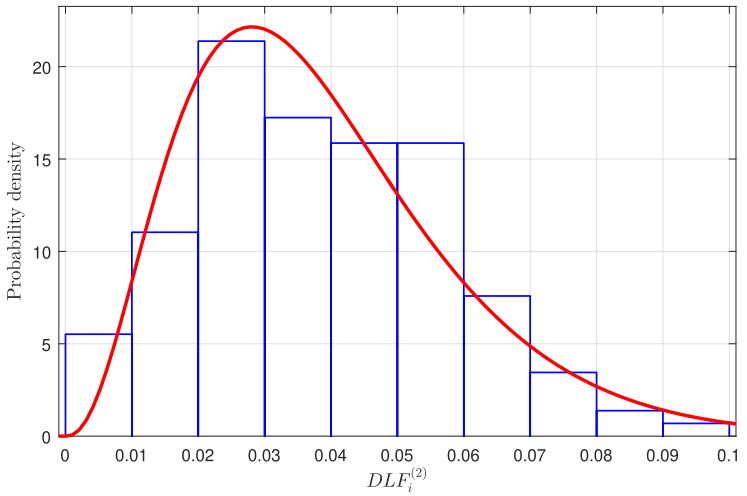

Fig. 3. Probability density of $DLF_i^{(2)}$. The data are the same as in Fig. 1. The histogram is derived from the experimental data, while the line is the fitted Beta distribution.

In a trial, μ and σ^2 can be approximated from its average $\overline{DLF}^{(j)}$ and $CoV^{(j)}$ as:

$$\mu \cong \overline{DLF}^{(j)}, \quad \sigma^2 \cong \left(\overline{DLF}^{(j)} \cdot CoV^{(j)}\right)^2. \tag{8}$$

To conclude, the sequence $DLF_i^{(j)}$ in a treadmill walking trial can be considered a random process described by a Beta distribution which parameters can be approximated using the average $\overline{DLF}^{(j)}$ and $CoV^{(j)}$ calculated form DLF data extracted from a measured GRF trial. Therefore, adequate mathematical descriptions of the average and CoV are essential to generate reliably an artificial sequence of DLFs. This is exactly what the next section aims to address.

3.2. Statistical modelling of DLF components

Fig. 4 shows a relationship between the average values $\overline{DLF}^{(j)}$ from each walking trial and the constant (treadmill) walking speed v. First of all, a visual inspection of the figure points to a significant degree of inter-pedestrian variability of the data. Moreover, all the graphs show apparently increasing trend of the DLF values as pedestrians walk faster. Although the trend becomes flatter for the higher (sub) harmonics, all the data can be described reliably by the following formulation:

$$\overline{DLF}^{(j)} = \overline{DLF}_d^{(j)}\ 10\ \overline{DLF}_r^{(j)}. \tag{9}$$

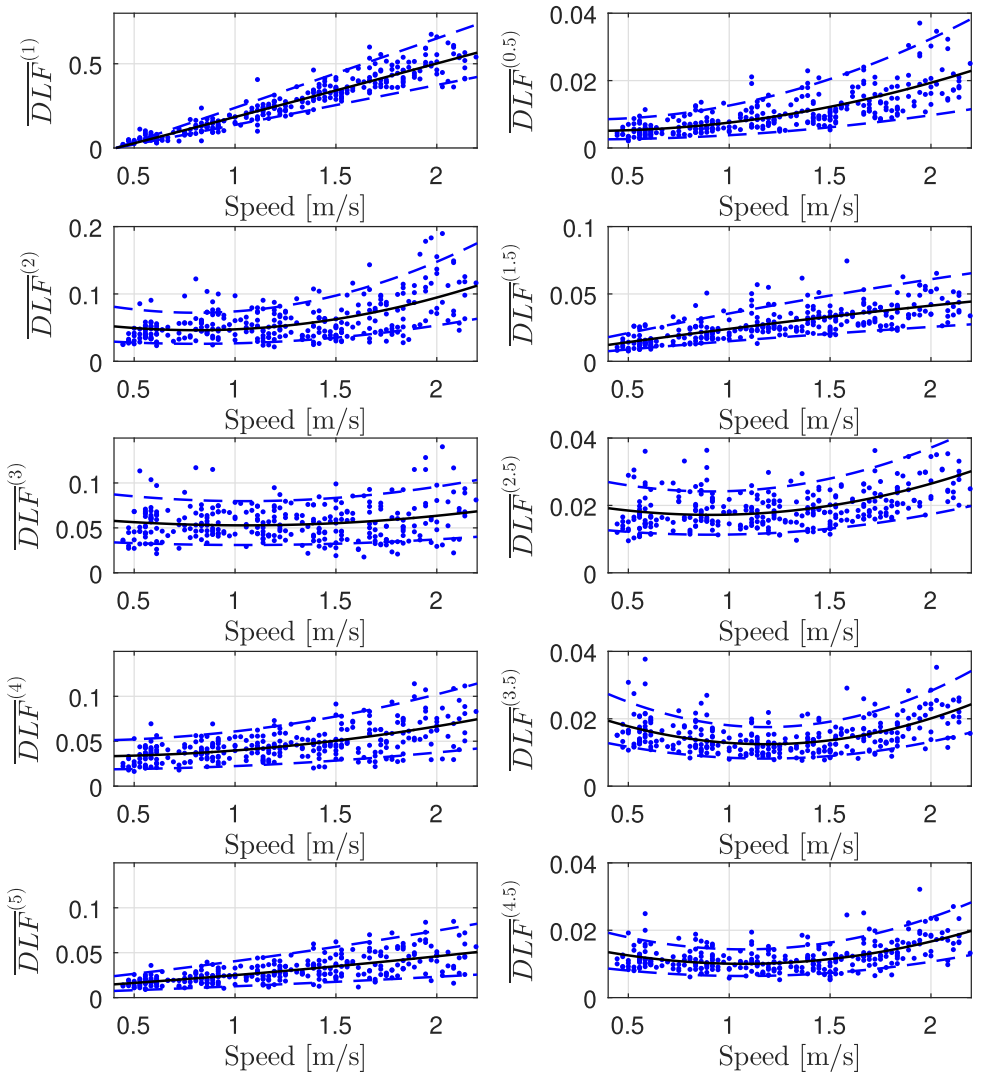

Fig. 4. $\overline{DLF}^{(j)}$ vs. walking speed v. The dots represent the data, the solid lines the quadratic fit and the broken lines the 95% confidence bounds.

The first factor $\overline{DLF}_d^{(j)}$ represents a deterministic component of $\overline{DLF}^{(j)}$, while the second factor $\overline{DLF}_r^{(j)}$ is a random variable which accounts for the inter-pedestrian variability. The deterministic factor describes the global increasing trend in the relationship $\overline{DLF}^{(j)}$ vs. v which can be mathematically modelled as a second-order polynomial:

$$\overline{DLF}_d^{(j)} = c_9^{(j)} v^2 + c_{10}^{(j)} v + c_{11}^{(j)}. \tag{10}$$

The values of the coefficients $c_9^{(j)}, c_{10}^{(j)}$ and $c_{11}^{(j)}$ were obtained by fitting the polynomial to the data shown in Fig. 4 and are reported in Table 2. The fits and 95% confidence intervals are shown in Fig. 4 together with the actual data.

The random factor $\overline{DLF}_r^{(j)}$ was calculated after substituting Eq. (10) into Eq. (9):

$$\overline{DLF}_r^{(j)} = \frac{\overline{DLF}^{(j)}}{10\left(c_9^{(j)} v^2 + c_{10}^{(j)} v + c_{11}^{(j)}\right)}. \tag{11}$$

Eventually, the value of $\overline{DLF}_r^{(j)}$ representative of each pedestrian was estimated as the average value of the related six experiments. The constant 10 in Eq. (9) limits values of the random factors to the range [0, 1]. In this way, the values fit well Beta distribution $\mathrm{B}(c_{12}, c_{13})$. The values of the parameters c_{12} and c_{13} listed in Table 2 were obtained using the maximum likelihood method [36].

The calculated CoVs of the DLF values are shown in Fig. 5. Apart from the first harmonic, the data show no apparent trend as walking speed increases. Therefore, they can be assumed uniformly distributed across the measured range of speeds. For the first harmonic, the data form a concave pattern with the minimum at the speed of approximately 1.7 m/s. This can be

Table 2
Parameter values of $\overline{DLF}^{(j)}$ model.

(Sub) harmonic order (j)	c_9	c_{10}	c_{11}	c_{12}	c_{13}
0.5	0.0049	−0.0028	0.0055	10.06	89.29
1	0.0037	0.3064	−0.1263	45.51	407.69
1.5	−0.0017	0.0222	0.0035	18.85	168.56
2	0.0341	−0.0551	0.0685	13.78	123.17
2.5	0.0077	−0.0140	0.0236	24.55	220.83
3	0.0118	−0.0246	0.0657	15.93	143.33
3.5	0.0114	−0.0270	0.0284	24.35	219.03
4	0.0103	−0.0039	0.0333	14.24	128.88
4.5	0.0077	−0.0164	0.0188	22.00	198.18
5	0.0024	0.0138	0.0089	10.66	96.85

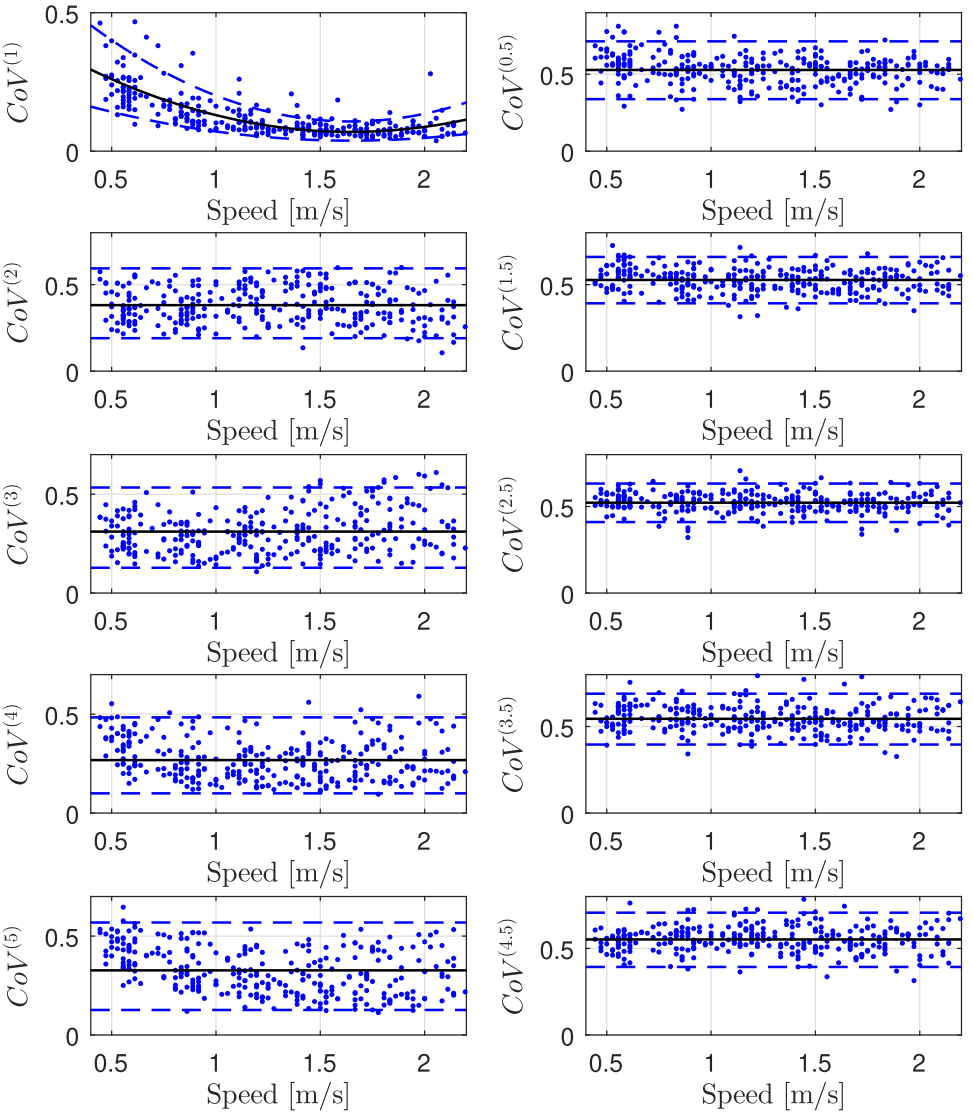

Fig. 5. $CoV^{(j)}$ vs. walking speed v. The dots represent the data, the solid lines the quadratic fit and the broken lines the 95% confidence bounds.

interpreted as the preferred walking speed at which the body energy expenditure is minimised [2]. The value is within the range reported in the relevant studies on energetic cost of walking [14].

Similar to the average values of $\overline{DLF}^{(j)}$, also $CoV^{(j)}$ can be described as the product of a deterministic factor $CoV_d^{(j)}$ and a random factor $CoV_r^{(j)}$:

$$CoV^{(j)} = CoV_d^{(j)}\ 10\ CoV_r^{(j)}. \tag{12}$$

Broadly speaking, the deterministic part can be modelled as a second-order polynomial:

$$CoV_d^{(j)} = c_{14}^{(j)} v^2 + c_{15}^{(j)} v + c_{16}^{(j)}. \tag{13}$$

The values of the coefficients $c_{14}^{(j)}, c_{15}^{(j)}$ and $c_{16}^{(j)}$ are reported in Table 3. Note that coefficients $c_{14}^{(j)}$ and $c_{15}^{(j)}$ are zero for all harmonics except the first, which means that the corresponding fit becomes just a constant flat line $CoV_d^{(j)} = c_{16}^{(j)}$.

The random component, $CoV_r^{(j)}$, is obtained by dividing the actual $CoV^{(j)}$ values by the deterministic part and the factor 10:

$$CoV_r^{(j)} = \frac{CoV^{(j)}}{10\left(c_{14}^{(j)} v^2 + c_{15}^{(j)} v + c_{16}^{(j)}\right)}. \tag{14}$$

Similar to $\overline{DLF}_r^{(j)}$, the value of $CoV_r^{(j)}$ corresponding to each pedestrian was estimated as the average value of the related six experiments. It was found that $CoV_r^{(j)}$ values fit well a Beta distribution, $\mathrm{B}(c_{17}, c_{18})$. The values of the parameters c_{17} and c_{18} are determined by the maximum likelihood method [36] and are reported in Table 3. The fits and the corresponding 95% confidence intervals are shown in Fig. 5 together with the actual data.

3.3. Synthetic DLF values

For a given sequence of variable footfall speeds in a walking trial, v_i, elaborated in Section 2.1, the corresponding sequence of variable (also called "adaptive" to speed) $DLF_i^{(j)}$ values is generated by the following algorithm:

1. Calculate the deterministic part of $\overline{DLF}^{(j)}$, $\overline{DLF}_{di}^{(j)} = c_9^{(j)} v_i^2 + c_{10}^{(j)} v_i + c_{11}^{(j)}$.
2. Sample $\overline{DLF}_r^{(j)}$ from $\mathrm{B}(c_{12}, c_{13})$.
3. Calculate the adaptive values for successive steps/strides, $\overline{DLF}_i^{(j)} = \overline{DLF}_{di}^{(j)}\ 10\,\overline{DLF}_r^{(j)}$.
4. Calculate the deterministic factor of $CoV^{(j)}$, $CoV_{di}^{(j)} = c_{14}^{(j)} v_i^2 + c_{15}^{(j)} v_i + c_{16}^{(j)}$.
5. Sample $CoV_r^{(j)}$ from $\mathrm{B}(c_{17}, c_{18})$.
6. Calculate $CoV^{(j)}$ for successive steps/strides, $CoV_i^{(j)} = CoV_{di}^{(j)}\ 10\ CoV_r^{(j)}$.
7. Compute mean and variance for each step/stride, $\mu_i^{(j)} = \overline{DLF}_i^{(j)}$, $\left(\sigma_i^{(j)}\right)^2 = \left(CoV_i^{(j)} \cdot \overline{DLF}_i^{(j)}\right)^2$.
8. Calculate parameters a_i and b_i of $DLF_i^{(j)}$ distribution of the (sub) harmonics in each (stride) step, $a_i^{(j)} = \frac{\left(\mu_i^{(j)}\right)^2\left(1-\mu_i^{(j)}\right)}{\left(\sigma_i^{(j)}\right)^2} - \mu_i^{(j)}$, $b_i^{(j)} = \frac{1-\mu_i^{(j)}}{\mu_i^{(j)}} a_i^{(j)}$.
9. Generate $DLF_i^{(j)}$ sequence by sampling from $\mathrm{B}(a_i^{(j)}, b_i^{(j)})$.

The first three steps of the algorithm create artificial DLF values which variation is "reduced" to the inter-pedestrian variability. The remaining steps add the intra-pedestrian variability, so such DLFs account for the actual top level of variability of the GRF amplitudes. The significance of this extra layer of variability to simulate reliably vibration response of a structure will be demonstrated in the next section.

Table 3
Parameter values of $CoV^{(j)}$ model.

(Sub) harmonic order (j)	c_{14}	c_{15}	c_{16}	c_{17}	c_{18}
0.5	0	0	0.1000	13.53	12.10
1	0.1450	−0.4773	0.4625	13.35	121.81
1.5	0	0	0.1000	27.33	24.54
2	0	0	0.1000	7.90	12.82
2.5	0	0	0.1000	39.65	36.29
3	0	0	0.1000	5.73	12.67
3.5	0	0	0.1000	23.24	19.41
4	0	0	0.1000	5.04	13.73
4.5	0	0	0.1000	20.53	16.62
5	0	0	0.1000	5.12	10.56

4. Model assessment and validation

This section gathers everything presented so far to demonstrate the validity of the proposed model to reliably simulate vibration response. In Section 4.1 amplitudes and trends of the synthetic DLFs generated as elaborated in the previous section will be compared with the DLFs reported elsewhere ([3,19]). Responses of an imaginary (fictive) footbridge due to experimentally measured and the corresponding synthetic walking forces featuring variable DLF amplitudes will be compared in Section 4.2 to examine how close they match. Further comparison between the responses due to simulated walking forces with a reduced and the top level of the step-by-step variability of DLFs will be elaborated in Section 4.3.

4.1. Comparison with other DLF studies

Fig. 6 shows widely popular deterministic DLF models of the first four walking harmonics derived by Kerr using single footfall GRFs recorded by a force plate [3]. Kerr fitted a third order polynomial curve to DLFs of the first harmonic as a function of walking frequency. DLF values of the other three higher order harmonics were found independent from the walking frequency, thus modelled as constants. Fig. 6 also shows synthetic DLF data from this study corresponding to the Kerr's models. They include only deterministic components of DLFs described by Eq. (10). As the equation features walking speeds, the corresponding walking frequencies were determined by the power law established in Section 2.3.1 and using the mean values of parameters c_3 and c_4 (see Eq. (3)).

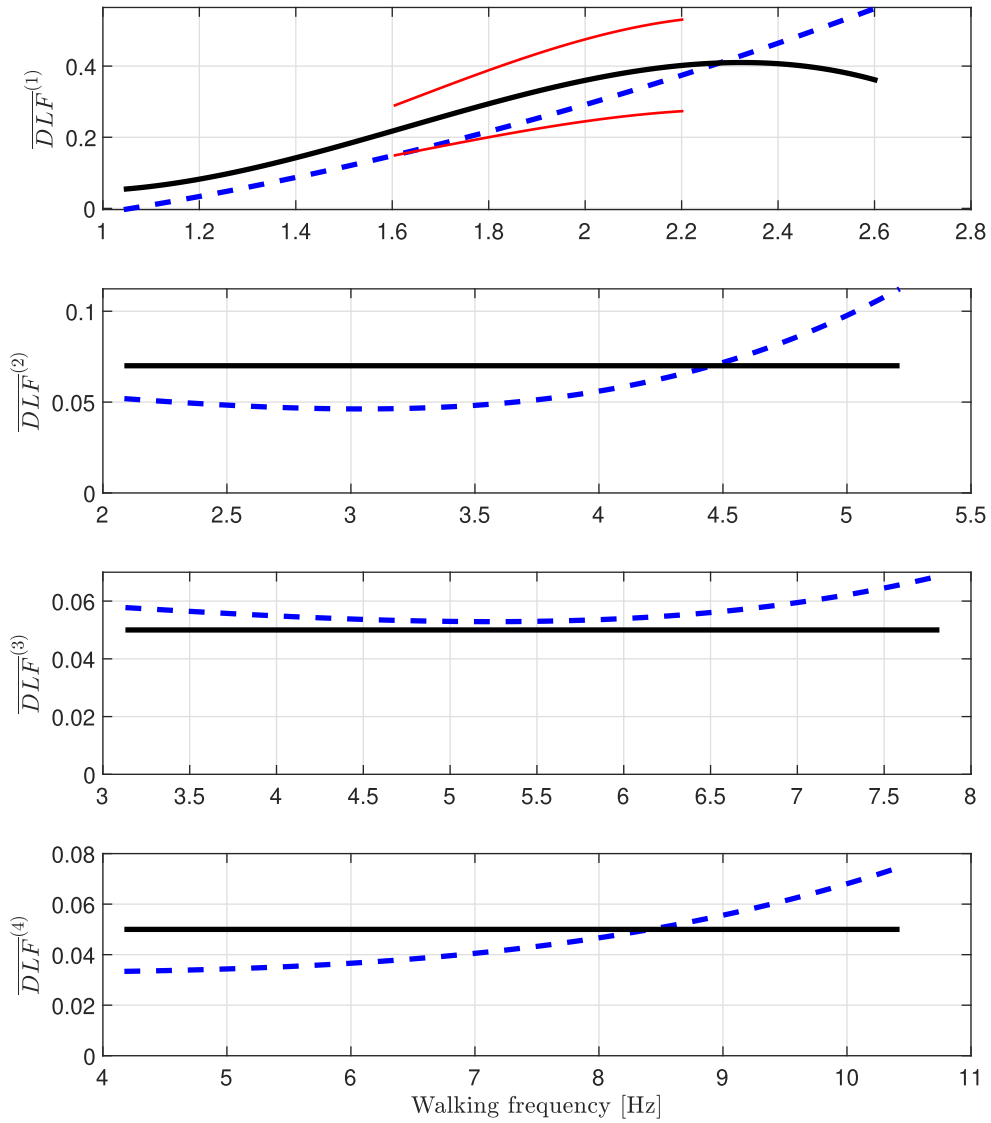

Fig. 6. $\overline{DLF}^{(j)}$ vs walking frequency. Solid lines: Kerr's study [3] Bold line: averages. Fine line: 95% confidence interval. Dashed lines: present study.

The plots relevant to the first harmonic show the same growing trend of DLFs as walking frequencies increase up to 2.3 Hz. The two curves run in parallel with a small offset of approximately 0.05. However, the present model is still within Kerr's 95% confidence interval. Above 2.3 Hz, the DLFs follow two opposite trends. Kerr's model suggests decreasing while the present model shows increasing DLF amplitudes with further increments of walking frequency. Nevertheless, Kerr himself noted that his results above 2.2 Hz are likely to be untrue due to a great level of data scarcity. For the higher harmonics, unlike Kerr's flat lines the present model features a light increasing trend in DLF values as pedestrians increase walking frequency. Again, the apparent differences are for pacing rates higher than approximately 2.3 Hz. Considering different experimental setups and the large scatter in the data points in both studies, the models generate fairly close results. The present study derived the DLFs from continuously measured treadmill walking including many successive footfalls per a walking trial rather than just a single footfall as collected by Kerr. Targeting a force plate during walking to avoid partial footfall measurements can alter natural gait pattern yielding unrealistic force records [2]. Moreover, the present study added a higher statistical rigor to the modelling by using around 30,000 data points, which is thirty times higher than in the Kerr's study.

DLFs derived from continuously measured force time histories as in this study are rare and limited. The values for the first five walking harmonics extracted by Kumar et al. [19] from treadmill force records generated by 12 test subjects (9 men and 3 women) at University of Sheffield are shown in Fig. 7. The average value of the dynamic load factors $\overline{DLF}^{(j)}$ from the present study together with their 95% confidence interval are added for comparison. Overall, the match is apparently closer than in case of the Kerr's model (Fig. 6). Increasing trends in DLF values are similar for all harmonics and most of the Sheffield data are within the confidence intervals. The best match is for the first harmonic, while some Sheffield DLFs are below the lower confidence border for the higher harmonics. However, more data points are needed to provide a more conclusive comparison. The reader should also bear in mind that the Sheffield experiments measured ethnically more diverse population of test subjects, while the treadmill records used in the present study included predominantly Spanish Caucasians.

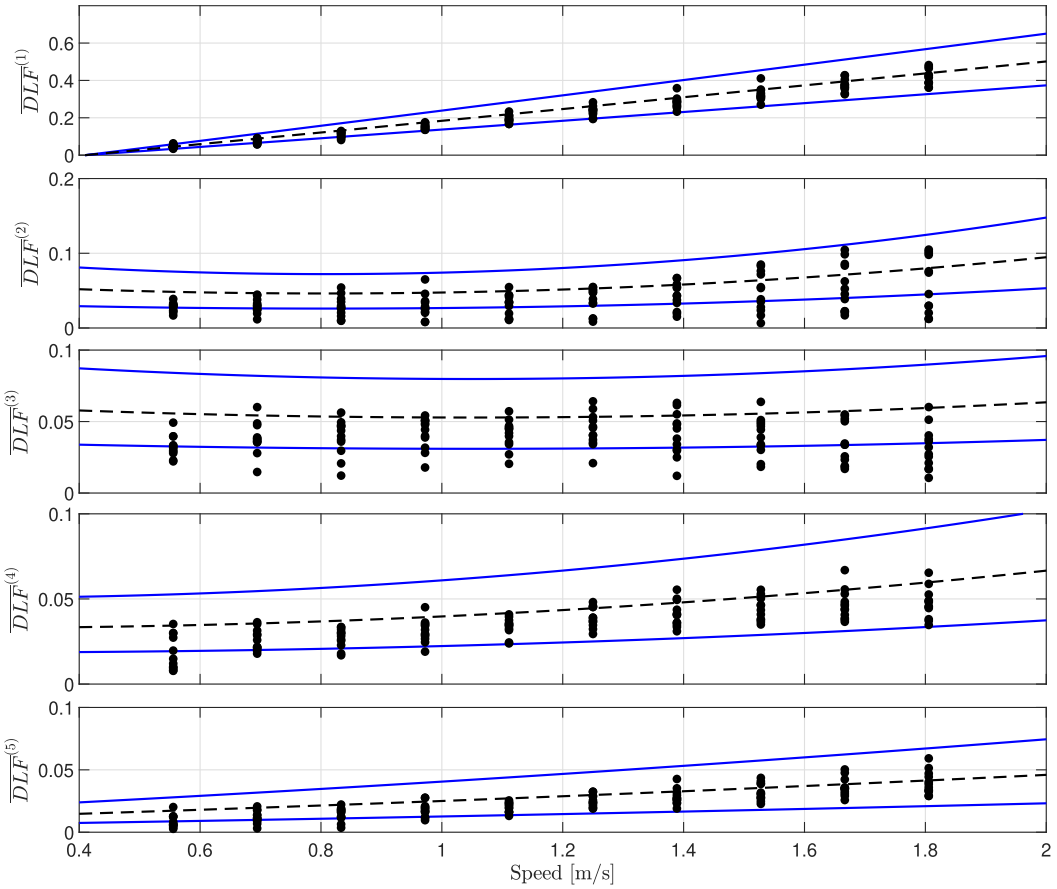

Fig. 7. $\overline{DLF}^{(j)}$ vs walking speed. Dashed lines represent average values, while solid lines are 95% confidence bounds. Dots are the results in [19].

4.2. Validation

4.2.1. Test structure and synthetic forces

The fictive footbridge is a 50 m long simple supported beam with the modal mass 1000 kg, damping ratio 0.5% and variable natural frequency in the range 0.6–12 Hz with step increments of 0.1 Hz. The frequency range is selected to mirror the range of frequencies covered by the force model. Only the first mode of vibration having a half-sine mode shape is considered in the simulations.

The vibration responses due to 50 treadmill forces measured for 50 individuals walking at their preferable speed were computed. To increase the statistical reliability of the validation, these forces were recorded separately from those used to derive the model. Next, each of the measured 50 forces was simulated 1000 times. Body weight W, walking speed v_i and step intervals T_i, were set equal to each measured force, while the corresponding sequence of DLFs was calculated following the algorithm presented in Section 3.3. Therefore, the simulated forces differ only by the sequence of DLFs values.

In vibration simulation walking forces was moving along the footbridge. The position of the force was computed through the procedure outlined in Section 2.3.4. As only one mode of vibration of the structure is taken into account, the phases of the force (sub) harmonics has a negligible effect on the response, so they are set to zero.

A total walking force signal is composed of three parts: due to harmonics $F_i^{(h)}(t)$, due to subharmonics $F_k^{(s)}(t)$ and due to the pedestrian's weight W. During a step $i, F_i^{(h)}(t)$ is mathematically characterised as:

$$F_i^{(h)}(t) = W \sum_{j=1,2,3,4,5} DLF_i^{(j)} \sin\left(\frac{2\pi j}{T_i} t\right), \quad (i = 1, 2, \ldots, N) \tag{15}$$

where t is time and $0 \leqslant t \leqslant T_i$.

The component $F_k^{(s)}(t)$ is characterised over a stride k as:

$$F_k^{(s)}(t) = W \sum_{j=0.5,1.5,2.5,3.5,4.5} DLF_k^{(j)} \sin\left(\frac{2\pi 2j}{T_k} t\right), \quad \left(k = 1, 2, \ldots, \frac{N}{2}\right) \tag{16}$$

in which t is within the limits $0 \leqslant t \leqslant T_k$.

As the total force signals are generated at discrete time steps Δt, the step intervals, T_i, are rounded to the minimum integer multiples of Δt.

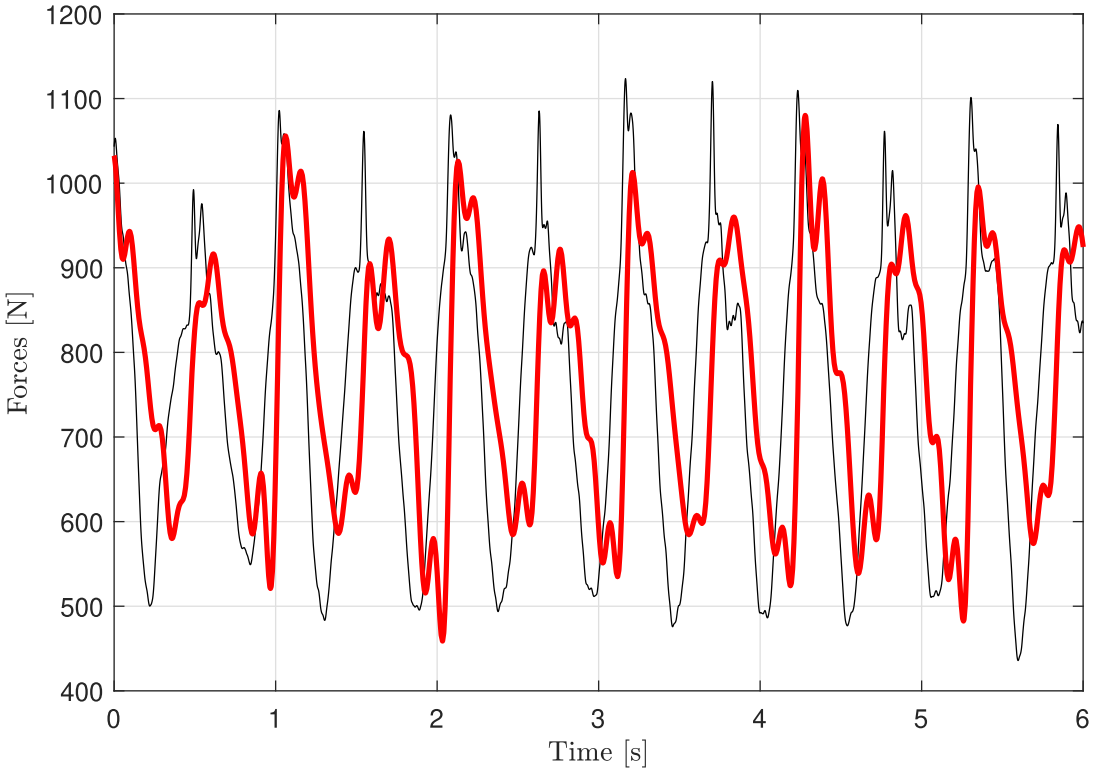

Fig. 8. Walking force signals. Fine line: experimental data. Bold line: synthetic counterpart.

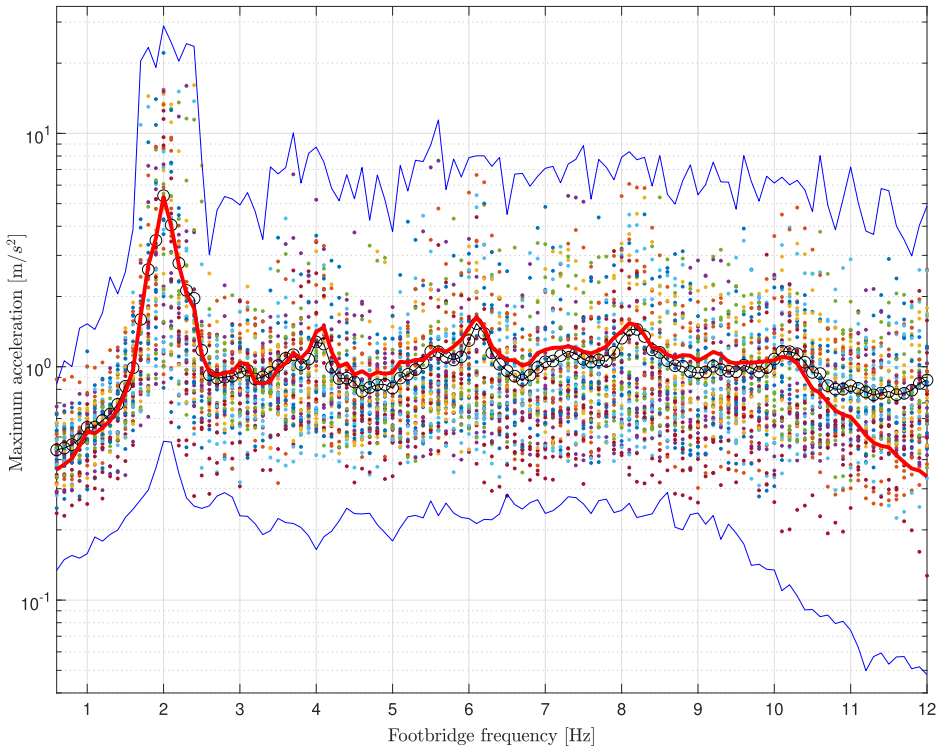

Fig. 9. Summary of simulation results. Dots represent peak accelerations due to experimental forces and circles are their averages. Fine (blue) lines are the upper and lower bounds of the peak accelerations due to the synthetic forces and the bold (red) line corresponds to their averages. (For interpretation of the references to colour in this figure legend, the reader is referred to the web version of this article.)

Fig. 8 shows a portion of measured force signal comprising 11 successive footfalls and a synthetic counterpart. Note that the signals differ as the (sub) harmonics in the synthetic force have zero phases. However, the variation is apparent and similar.

4.2.2. Results of vibration simulations

Fig. 9 shows peak accelerations of the virtual bridges due to each measured and simulated force signal. For each footbridge frequency, the average and extreme values of the simulated responses are highlighted for comparison. The average plots show apparent peaks at integer multiples of around 2 Hz and visible peaks at the frequencies in-between. These correspond to the force harmonics and subharmonics, respectively. Moreover, this means that the average pacing rate corresponding to the selected preferable walking speed was about 2 Hz for all test subjects, which is in line with findings reported elsewhere [2]. Fig. 9 shows highly satisfactory match between the results due to the actual and artificial forces for the footbridge natural frequencies approximately up to 10 Hz. The results start to part for the higher frequencies. This is because the force model accounts for the first five dominant harmonics (i.e. integer multiples of pacing rate) and subharmonics and the mean pacing rate was around 2 Hz. Moreover, this shows that the energy of the frequency content of the actual near-periodic forces above the fifth dominant harmonic still can induce notable vibrations, which was also observed by others [25]. However, it was argued in the literature [15,5] that this is the limit above the Fourier modelling approach stops to provide reasonable results. The results in Fig. 9 show that the present force model can predict both resonant and non-resonant vibration response for natural frequencies of footbridges up to 10 Hz.

In the so established frequency range 0–10 Hz, the capacity of the model to reliably simulate the experiments was studied by comparing acceleration responses due to each of 50 measured signals and the corresponding 1000 synthetic counterparts. Results relevant to one measured force are shown in Fig. 10. This is an example where 96% of the peak accelerations due to the measured force (bold plot) is within the extreme peak accelerations due to the artificial forces (fine lines) across the whole range of different footbridge natural frequencies. Even when outside the extreme value borders, the measured data is very close to the border. Similar graphs due to the remaining 49 measured forces show even better results. Namely, 97% of 4750 studied combinations of 50 pedestrian forces and 95 footbridges are fully within the borders.

4.3. The importance of intra-pedestrian variability

The shape and modal properties of the imaginary footbridges used in the vibration simulations carried out in this section were set equal to those from the previous section. However, walking of individuals was modelled as unrestricted, i.e. with

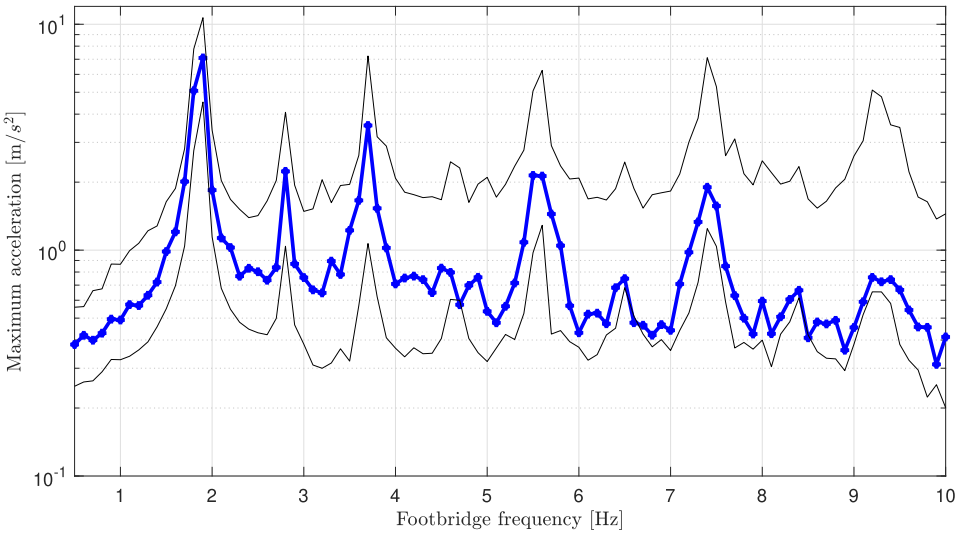

Fig. 10. Peak acceleration responses relevant to one measured force signal. Bold lines connect the data due to the measured signal, while thin lines are the minimum and maximum peak responses due to synthetic forces.

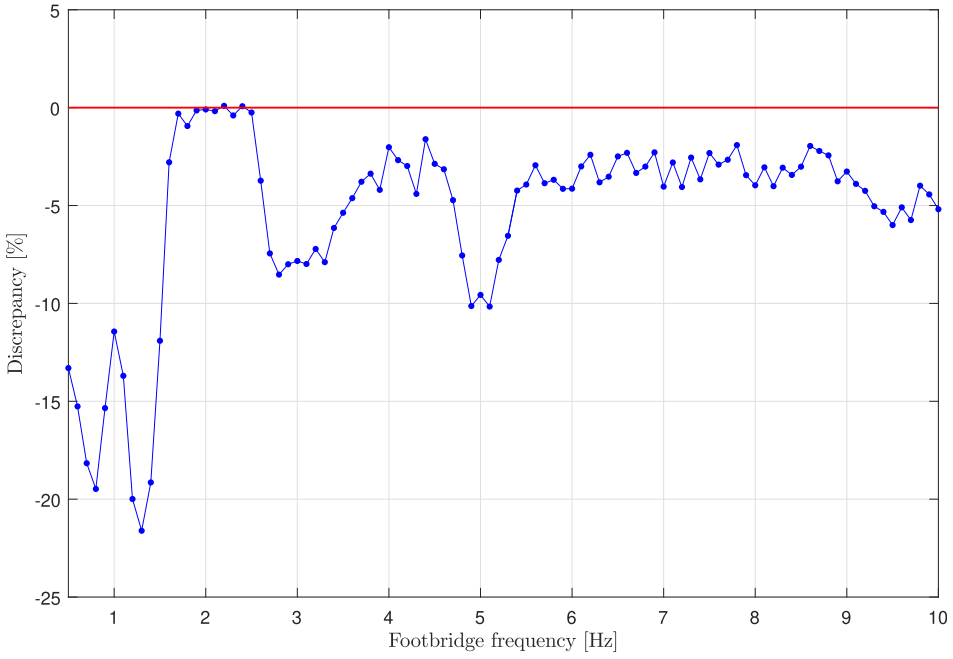

Fig. 11. Relative error between vibration responses due to the forces with reduced and top level variability of DLFs.

the variable speed on the step-by-step basis. The mean μ_v and standard deviation σ_v of the average walking speed in a trial were set to 1.4 m/s and 0.14 m/s, respectively. These are in the range of preferable (i.e. self-selected) walking speeds [2] and correspond to the mean walking frequency 2.05 Hz and standard deviation 0.19 Hz [21]. Hence, the resonant vibration response would be due to one of the corresponding five harmonics or five sub-harmonics of walking GRF. The pedestrian weight was assumed to have a Gaussian distribution with the mean 750 N and standard deviation 150 N.

Two series of 10,000 force time histories were generated with reduced and top level of DLF variability using the same sequence of step speeds v_i, step intervals T_i, pedestrian weight W, and adaptive DLF component $\overline{DLF}_i^{(j)}$. In this way, a comparison between the pairs of the corresponding vibration responses could highlight the effect of the intra-pedestrian vari-

ability of DLFs on the simulated vibration levels. Maximum accelerations were extracted from each series of 10,000 simulations. Then they were sorted in ascending order and 95% quantiles were estimated from the 9500:10,000 order statistic [37]. The relative errors between the corresponding 95% quantiles are shown in Fig. 11.

Broadly speaking, artificial forces with reduced DLF variability underestimate the vibration response. Within the range of the fundamental force harmonic [1.7–2.5] Hz, there is no notable difference. However, the relative error becomes larger (i.e. up to 10%) as the order of harmonics increases. The corresponding frequency ranges in Fig. 11 are $j \times [1.7—2.5]$ Hz, $j = 2, \ldots, 5$. This is because intra-pedestrian DLF variability of the higher harmonics is up to four times that of the fundamental harmonic. The dips in Fig. 9 are more prominent in the frequency range of the subharmonics, $0.5 \times j \times [1.7—2.5]$ Hz. These show the relative error between 8.5 and 20%. Outside the frequency ranges of the force harmonics and sub-harmonics the error is as high as 22%. Note that vibration response in this case is not resonant.

5. Discussion and conclusions

The key novelty of the model developed in this study is that it creates stochastic walking force signals where all modelling parameters are functions of variable walking speed on the step-by-step basis. This is a radical departure from traditionally used deterministic models which generate periodic force time histories and where the key modelling parameters are functions of the average pacing rate in a walking trial. Walking speed rather than pacing rate is a more natural choice of the input variable as human nervous system adopts speed of successive steps to the surrounding environment and different circumstances, such as vibration of the supporting ground. Moreover, crowded situations are the most relevant loading scenarios where the speed of individual pedestrians is more or less controlled by the crowd flow and the crowd density.

This study started from the previously developed models describing both inter- and intra-pedestrian variability of walking speed and spatiotemporal parameters in a walking trial. Then it delivered a complementary model of variable DLFs corresponding to the first five dominant harmonics and subharmonics of the walking force. Although Kerr studied the first four harmonics only based on single footfall data [3], his deterministic DLF values are in line with the corresponding DLF values derived in the present study from continuously measured force time histories. Both the mean and CoV of DLFs are described as the products of two factors. The first represents the deterministic dependence on the step speed and is modelled as a second-order polynomial. The second factor stands for the random inter-pedestrian variability of the DLFs and it is defined by a Beta distribution. Finally, all the relevant models could be integrated in a comprehensive model of artificial walking force signals where both pacing rate and force amplitudes vary on the step-by-step basis as functions of the variable step speed.

Results of extensive numerical simulations of vibration response of virtual footbridges showed little difference between the peak accelerations due to the actual and the equivalent artificial walking forces. Moreover, the results provided a strong argument for including intra-pedestrian variability of gait into a reliable model of pedestrian loading. In comparison with inter-pedestrian variability, this important attribute of individual walking excitation is unfairly disregarded in the civil engineering context yielding in this study errors in predicted vibration response as high as 22%.

This study has several limitations, mainly due to the lack of the relevant data. It focusses to pedestrian loading induced by individuals only, while a more relevant load case scenario (particularly for footbridges) is a constant flow of pedestrians. It gets even more complicated in case of dense crowds when gait of individuals is affected by a proximity of surrounding people. People are social beings who mutually interact through different combinations of visual, audio and tactile cues. How these external (social) stimuli influence the walking forces remains unanswered. However, an error as high as 22% just due to neglecting intra-pedestrian variability seems unlikely for pedestrian streams. Still, rare studies based on experimental measurements and numerical simulations of footbridge vibrations due to multiple pedestrian occupants argued that intra-pedestrian variability of walking deserves comparable attention as external cues [11,12].

The walking forces used to derive the force model are recorded on a “rigid” ground. So, it also remains unknown to which extent the vertical footfall forces studied here are close to those generated on more or less flexible surfaces. Moreover, the force recordings took place in a controlled laboratory environment. Forces recorded on real structures might show a different level of step-by-step variability. Finally, the model is applicable to flat structures, such as footbridges without a dominant cumber or slabs without a slope, as the walking forces on horizontal and inclined surfaces are different [2]. However, the modelling approach is not restricted to the kind of force records analysed in this study. In contrary, the model can fit a wider range of measured walking force signals recorded under above mentioned and currently unexplored circumstances as soon as they have been made available.

CRediT authorship contribution statement

M. García-Diéguez: Data curation, Formal analysis, Project administration, Software, Visualization, Validation, Funding acquisition. **V. Racic:** Investigation, Validation, Writing - original draft, Writing - review & editing. **J.L. Zapico-Valle:** Conceptualization, Formal analysis, Funding acquisition, Methodology, Supervision.

Declaration of competing interest

The authors certify that they have NO affiliations with or involvement in any organization or entity with any financial interest, or non-financial interest in the subject matter or materials discussed in this manuscript.

Acknowledgements

The authors would like to thank all the voluntaries for their generous help to collect the experimental data used in this study. The financial support provided by the Spanish Ministry of Economy and Competitiveness through project PGC2018-096670-B-100 is specially acknowledged.

References

[1] S. Živanović, A. Pavic, P. Reynolds, Vibration serviceability of footbridges under human-induced excitation: a literature review, J. Sound Vib. 279 (2005) 1–74.
[2] V. Racic, J.M.W. Brownjohn, Experimental identification and analytical modelling of human walking forces: Literature review, J. Sound Vib. 326 (2009) 1–49.
[3] S.C. Kerr, Human Induced Loading on Staircases PhD Thesis, University College London, Mechanical Engineering Department, London, UK, 1998.
[4] J.M.W. Brownjohn, A. Pavic, P. Omenzetter, A spectral density approach for modelling continuous vertical forces on pedestrian structures due to walking, Can. J. Civ. Eng. 31 (2004) 65–77.
[5] V. Racic, J.M.W. Brownjohn, Stochastic model of near-periodic vertical loads due to humans walking, Adv. Eng. Inf. 25 (2011) 259–275.
[6] V. Racic, J.M.W. Brownjohn, Mathematical modelling of random narrow band lateral excitation of footbridges due to pedestrians walking, Comput. Struct. 90–91 (2012) 116–130.
[7] M. Kasperski, C. Sahnaci, Serviceability of pedestrian structures, Conference Proceedings of the Society for Experimental Mechanics Series (IMAC XXV) (2007)..
[8] J. Chen, G. Ding, S. Živanović, Stochastic single footfall trace model for pedestrian walking load, Int. J. Struct. Stab. Dyn. 19 (3) (2019).
[9] M. Bocian, J.H.G. Macdonald, J.F. Burn, Biomechanically inspired modeling of pedestrian-induced vertical self-excited forces, J. Bridge Eng. 18 (12) (2013) 1336–1346.
[10] H.V. Dang, S. Živanović, Experimental characterisation of walking locomotion on rigid level surfaces using motion capture system, Eng. Struct. 91 (2015) 141–154.
[11] K. Van Nimmen, G. Zhao, A. Seyfarth, P. Van den Broeck, A robust methodology for the reconstruction of the vertical pedestrian-induced load from the registered body motion, Vibration 1 (2) (2018) 250–268.
[12] M. Bocian, J.M.W. Brownjohn, V. Racic, D. Hester, A. Quattrone, R. Monnickendam, A framework for experimental determination of localised vertical pedestrian forces on full-scale structures using wireless attitude and heading reference systems, J. Sound Vib. 376 (2016) 217–243.
[13] Z. Feng, L. Shao, V. Racic, J.M.W. Brownjohn, Measuring human-induced vibrations of civil engineering structures via vision-based motion tracking, Measurement 83 (2016) 44–56.
[14] J. Rose, J.G. Gamble, Human Walking, second ed., Williams & Wilkins, Baltimore, 1994.
[15] S. Živanović, A. Pavic, Probabilistic modelling of walking excitation for building floors, J. Perform. Construct. Facilit. 23 (3) (2009) 132–143.
[16] F. Tubino, Probabilistic assessment of the dynamic interaction between multiple pedestrians and vertical vibrations of footbridges, J. Sound Vib. 417 (2018) 80–96.
[17] F. Venuti, V. Racic, A. Corbetta, Modelling framework for dynamic interaction between multiple pedestrians and vertical vibrations of footbridges, J. Sound Vib. 379 (2016) 245–263.
[18] M.R. Willford, P. Young, A Design Guide for Footfall Induced Vibration of Structures CCIP-016, The Concrete Centre, Slough, 2006.
[19] P. Kumar, A. Kumar, V. Racic, S. Erlicher, Modelling vertical human walking forces using self-sustained oscillator, Mech. Syst. Sig. Process. 99 (2018) 345–363.
[20] M. Bocian, J.M.W. Brownjohn, V. Racic, D. Hester, A. Quattrone, L. Gilbert, R. Beasly, Time-dependent spectral analysis of interactions within groups of walking pedestrians and vertical structural motion using wavelets, Mech. Syst. Sig. Process. 105 (2018) 502–523.
[21] M. García-Diéguez, J.L. Zapico-Valle, Sensitivity of the vertical response of footbridges to the frequency variability of crossing pedestrians, Vibration 1 (2) (2018) 290–311.
[22] S.H. Collins, A.D. Kuo, Two Independent Contributions to Step Variability during Over-Ground Human Walking, Plos one Open access 8 (8) (2013) e73597.
[23] M. García-Diéguez, J.L. Zapico-Valle, Statistical modelling of spatiotemporal variability of overground walking, Mech. Syst. Sig. Process. 129 (2019) 186–200.
[24] M. García-Diéguez, J.L. Zapico-Valle, Statistical modeling of the relationships between spatiotemporal parameters of human walking and their variability, J. Struct. Eng. 143 (12) (2017) 04017164.
[25] A. Mohammed, A. Pavic, V. Racic, Improved model for human induced vibrations of high-frequency floors, Eng. Struct. 168 (2018) 950–966.
[26] C.C. Caprani, E. Ahmadi, Formulation of human-structure interaction system models for vertical vibration, J. Sound Vib. 377 (2016) 346–367.
[27] E. Shahabpoor, A. Pavic, V. Racic, S. Živanović, Effect of group walking traffic on dynamic properties of pedestrian structures, J. Sound Vib. 387 (2017) 207–225.
[28] S. Živanović, Benchmark footbridge for vibration serviceability assessment under the vertical component of pedestrian load, J. Struct. Eng. 138 (2012) 1193–1202.
[29] A. Pachi, T. Ji, Frequency and velocity of people walking, Struct. Eng. 83 (2005) 36–40.
[30] S. Chandra, A.K. Bharti, Speed distribution curves for pedestrians during walking and crossing, Procedia Soc. Behav. Sci. 104 (2013) 660–667.
[31] P.O. Riley, G. Paolini, U.D. Croce, K.W. Paylo, D.C. Kerrigan, A kinematic and kinetic comparison of overground and treadmill walking in healthy subjects, Gait Posture 26 (1) (2007) 17–24.
[32] M. van de Putte, N. Hagemeister, N. St-Onge, G. Parent, J.A. de Guise, Habituation to treadmill walking, Bio-Med. Mater. Eng. 16 (2006) 43–52.
[33] S.J. Lee, J. Hidler, Biomechanics of overground vs. treadmill walking in healthy individuals, J. Appl. Physiol. 104 (2008) 747–755.
[34] L.H. Sloot, M.M. van der Krogt, J. Harlaar, Self-paced versus fixed speed treadmill walking, Gait Posture 39 (1) (2014) 478–484.
[35] J.H. Hollman, M.K. Watkins, A.C. Imhoff, C.E. Braun, K.A. Akervik, D.K. Ness, A comparison of variability in spatiotemporal gait parameters between treadmill and overground walking conditions, Gait Posture 43 (2016) 204–209.
[36] V.K. Rohatgi, A.K.Md. Ehsanes Saleh, An Introduction to Probability and Statistics, John Wiley & Sons, 2011.
[37] E. Castillo, A.S. Hadi, N. Balakrihnan, J.M. Sarabia, Extreme Value and Related Models with Applications in Engineering and Science, Wiley-Interscience, New Jersey, USA, 2004.